










AKADÉMIAI KIADÓ

The role of imaging in the diagnosis and management of idiopathic pulmonary fibrosis

IMAGING

CHIARA NARDOCCI¹ , JUDIT SIMON^{1,2} , FANNI KISS³,
TAMÁS GYÖRKE³ , PÉTER SZÁNTÓ¹,
ÁDÁM DOMONKOS TÁRNOKI^{1,4} ,
DÁVID LÁSZLÓ TÁRNOKI^{1,4} , VERONIKA MÜLLER⁵  and
PÁL MAUROVICH-HORVAT^{1,2*} 

¹ Department of Radiology, Medical Imaging Centre, Semmelweis University, Budapest, Hungary

² MTA-SE Cardiovascular Imaging Research Group, Heart and Vascular Center, Semmelweis University, Budapest, Hungary

³ Department of Nuclear Medicine, Medical Imaging Centre, Semmelweis University, Budapest, Hungary

⁴ National Institute of Oncology, Budapest, Hungary

⁵ Department of Pulmonology, Semmelweis University, Budapest, Hungary

REVIEW ARTICLE



Received: May 20, 2021 • Accepted: August 9, 2021

ABSTRACT

Idiopathic pulmonary fibrosis (IPF) is a chronic progressive disease lacking a definite etiology, characterized by the nonspecific symptoms of dyspnea and dry cough. Due to its poor prognosis, imaging techniques play an essential role in diagnosing and managing IPF. High resolution computed tomography (HRCT) has been shown to be the most sensitive modality for the diagnosis of pulmonary fibrosis. It is the primary imaging modality used for the assessment and follow-up of patients with IPF. Other not commonly used imaging methods are under research, such as ultrasound, magnetic resonance imaging and positron emission tomography-computed tomography are alternative imaging techniques. This literature review aims to provide a brief overview of the imaging of IPF-related alterations.

KEYWORDS

computed tomography, interstitial lung disease, positron emission tomography, pulmonary fibrosis, ultrasound, usual interstitial pneumonia

Introduction

Idiopathic pulmonary fibrosis (IPF), a type of interstitial lung disease (ILD), is a chronic, progressive and ultimately fatal fibrosing lung disease of unknown cause presenting itself with a usual interstitial pneumonia (UIP) pattern [1]. To diagnose, a thorough medical history, laboratory evaluation and imaging are compulsory, sometimes even requiring pathological input. Due to its poor prognosis, radiologists play an essential role in diagnosing and managing IPF. Accurate diagnosis is essential for the introduction of the required antifibrotic therapies [2]. For instance, immunosuppressive drugs used in the therapy of other ILDs are in turn harmful for IPF patients [3].

The guidelines and imaging classification schemes for the diagnosis of IPF were created in 2011 based on a collaborative accord of the American Thoracic Society (ATS), European Respiratory Society (ERS), Japanese Respiratory Society (JRS) and Latin American Thoracic Association (ALAT) [1]. In 2018, two addendums were made by the same international societies and added them to the already existing guidelines, along with the Fleischner Society's white paper as an updated approach [4].

IMAGING (2021)

DOI: [10.1556/1647.2021.00048](https://doi.org/10.1556/1647.2021.00048)

© 2021 The Author(s)

*Corresponding author.

E-mail: maurovich-horvat.pal@med.semmelweis-univ.hu



This literature review aims to provide a brief overview of IPF, focusing on the diagnostic power that imaging techniques provide in the definite diagnosis of IPF and as an aid contributing to the multidisciplinary diagnostic (MDD) process.

Epidemiology

IPF is the most common form of ILD, affecting approximately 3 million people worldwide [5]. The incidence is higher in North America and Europe, 3 to 9 cases per 100,000 person-years, than in South America and East Asia, presenting fewer than 4 cases per 100,000 person-years [6]. The majority of the patients affected are over the age of 65 and predominately male. The prevalence and incidence have shown to increase over the last decade, questioning if in earlier studies there was an underestimation due diagnosing uncertainty. Its prognosis is worse than that of most cancers [2]. IPF accounts for 15–30% of ILD and most deaths are associated with respiratory failure or complications due to comorbidities [7].

There is lack of adequate evidence portraying the definite etiology of IPF. Comorbidities such as pulmonary hypertension, chronic obstructive pulmonary disease (COPD), lung cancer, obstructive sleep apnea, ischemic heart disease and gastroesophageal reflux (GERD) have shown correlation to its development [5]. One single center study demonstrated that 12% of patients with IPF had no comorbid illnesses, 58% of patients had 1–3 and 30% had 4–7 comorbidities [8]. The EMPIRE registry with 1620 IPF patients enrolled, illustrates age (71.4% male) and smoking history (62.9%) as the strongest demographic risk factors [9]. Regardless of their risk factors, all IPF patients are mechanistically similar in the development of their pathology. Due to this limitation, the survival, although variable from patient to patient, is estimated to have a median of 3–5 years if left untreated [5].

Pathophysiology

IPF is mainly a restrictive lung disease, stemming from an ongoing repair process resulting in excess collagen scar tissue in the interstitium of the lung. The aberrant deposition of extracellular matrix, characterized by various patterns of inflammation, leads to extensive lung remodeling and fibrosis [2]. Triggers of this chronic repair process lead to a progressive loss of lung tissue and gas exchange abnormalities. Normally, when the alveoli lining is damaged, type I pneumocytes secrete TGF β 1, resulting in type II pneumocytes further stimulating fibroblasts to divide and proliferate into myofibroblasts [2]. Subsequently, once myofibroblasts secrete reticular fibers as their repair process, they undergo apoptosis. In IPF patients however, when this process is triggered, the problem arises because type II pneumocytes over-proliferate during the repair process, resulting in too many myofibroblasts and the over-production of collagen. In addition, the myofibroblasts do not

undergo apoptosis; they continue to produce collagen causing a thickening of the interstitial space between the alveoli and the capillary. Thus, the aberrant reparative response to repetitive alveolar epithelial injury causes the stochastic pro-fibrotic reprogramming, premature and persistent epithelial senescence, and excessive production of mesenchymal cells which instigate a maladaptive response leading to the development of IPF [5]. The lungs in turn become stiff, and a restricted lung expansion due to fibrosis of the interstitium develops. The excess collagen also leads to the loss of the alveoli, creating fluid filled spaces or cysts, surrounded by thick walls, in a pattern called honeycombing. It is a progressive process, meaning that the symptoms will worsen over time. Oxygenation and ventilation problems cause clinical symptoms of coughing and shortness of breath, cyanosis and digital clubbing. Over time this leads to respiratory failure as the lungs lose healthy and functional tissue. Secondary traction bronchiectasis a hallmark sign in IPF and often observed concomitant emphysema results in obstructive ventilatory abnormalities hiding the restrictive ventilatory pattern of the fibrosing lungs.

Symptoms and diagnostic steps

IPF usually presents itself with nonspecific symptoms. Progressive dyspnea on exertion with dry cough, bibasilar crackles and finger clubbing occurs in 20–50% of patients. Cyanosis and right ventricular failure signs are seen in advanced stages [10]. Initial symptoms are attributed to aging, deconditioning or other comorbidities related to emphysema or cardiovascular disease. IPF patients are commonly seen to carry comorbidities. The most common ones being GERD, COPD and coronary artery disease [11]. Disease progression varies among patients. Slow progression, rapid progression, acute exacerbation and patient survival after an acute exacerbation, are behaviors in which imaging can play a crucial role in predicting outcome. The diagnosis of IPF depends on the exclusion of other ILDs. When an underlining etiology supporting the pathophysiological changes in the lung is absent, IPF is characterized based on the presence of radiographic and/or histopathological pattern of UIP.

UIP presents with:

1. Honeycombing pattern – subpleural air-filled cysts with well-defined thick walls
2. Traction bronchiectasis – dilated bronchi due to pulling of nearby fibrotic alveoli
3. Peripheral alveolar septal thickening – reticular pattern with network of fine lines

UIP is seen mostly bilaterally, peripherally and with basal reticular abnormality distribution. IPF is thought to first present itself in the base and periphery of the lungs, progressing to convolve the entirety of the lung tissue [5, 10].

For patients presenting with basilar crackles and unexplained symptomatic or asymptomatic basilar fibrosis on chest x-ray, a high resolution computed tomography (HRCT) is recommended [4]. Serological testing is taken to exclude any sort of connective-tissue associated diseases as



Table 1. The steps of the diagnosis of IPF

Medical history	<ul style="list-style-type: none"> ->65 years old -History of smoking -Exertional dyspnea -Dry cough
Physical examination	<ul style="list-style-type: none"> -Velcro-like basilar inspiratory fine crackles -Digital clubbing -Acrocyanosis in severe cases
Pulmonary function test	<ul style="list-style-type: none"> -Reduced TLC -Reduced or normal FVC -FEV1 can be normal or slightly reduced -Impaired gas exchange, reduced DL_{co} -Exercise induced hypoxemia, followed by resting hypoxemia in end-stages
Laboratory tests	Autoimmune antibodies, CRP, CBC and liver
Chest X-ray	Bilateral basal reticular abnormalities or no significant changes
HRCT	UIP pattern, probable UIP pattern, indeterminate for UIP pattern or alternative diagnosis
Histology	Bronchoscopy BAL and/or SLB

Abbreviations: BAL = Bronchoalveolar lavage; CBC = Complete blood count; CRP = C-reactive protein; DL_{co} = Diffusing capacity for carbon monoxide; FEV1 = Forced expiratory volume; FVC = Forced expiratory volume; HRCT = High resolution computed tomography; PFT = Pulmonary functional test; SLB = Surgical lung biopsy; TLC = Total lung capacity; UIP = Usual interstitial pneumonia.

potential causes of ILD [4]. Table 1 highlights the steps in the diagnosis of IPF [2].

Diagnosis of IPF must be carefully assessed to avoid any confounding secondary causes for pulmonary fibrosis. The ascertainment of IPF is a challenge, as individuals may also present with atypical HRCT patterns. But it is clinically relevant to make a precise diagnosis to direct the pharmacological therapy needed. The diagnostic criteria of previously defined HRCT UIP patterns (ATS/ERS/JRS/ALAT classification) have been updated to definite UIP, probable UIP, indeterminate UIP and alternate diagnosis. The latter 3 have conditional recommendations to do bronchoalveolar lavage (BAL) and surgical lung biopsy (SLB). Performing a surgical biopsy is not recommended in patients illustrating a definite UIP [4]. Patients who demonstrate probable UIP and have a clinical context suggesting IPF, may avoid SLB. On the other hand, patients who demonstrate probable UIP without having any suggestive clinical context are suggested to undergo SLB. However, each patient must be assessed individually before such a procedure [12].

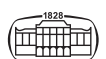
Histological UIP is seen as an interstitial fibrosis with spatial heterogeneity and patchy involvement of the lung parenchyma. Marked fibrotic areas and architectural distortion are also seen, with microscopic honeycombing. Proliferating aggregations of fibroblasts and myoblasts within a myxoid appearing matrix, called fibroblast foci, are the key histopathological feature of UIP [5].

Imaging modalities for the assessment of IPF

The use of imaging modalities leads to a better stratification of the disease, which is fundamental to individualize management and therapeutic strategies.

HRCT

For the definite diagnosis of IPF, UIP must be identified with HRCT. HRCT has specific and broad agreements in the definition of IPF patterns, illustrating fibrotic patterns of reticulation, traction bronchiectasis, honeycombing and ground-glass opacity (GGO) [13]. The HRCT criteria for the diagnosis of UIP are illustrated in Fig. 1. It is characterized by subpleural, basal predominance and reticular abnormality. GGO appears with preserved defined underlying structures, denoting a smaller attenuation increase [13]. Honeycombing (with or without traction bronchiectasis) is a characteristic that distinguishes the definite UIP pattern and probable UIP pattern. The diagnostic criteria for the description of IPF by HRCT and histological patterns by the 2018 ATS/ERS/JRS/ALAT Clinical Practice Guideline can be seen in Tables 2 and 3 [4, 14]. Reticular abnormality is a collection of innumerable small linear opacities resulting in a pattern that resembles a net, which



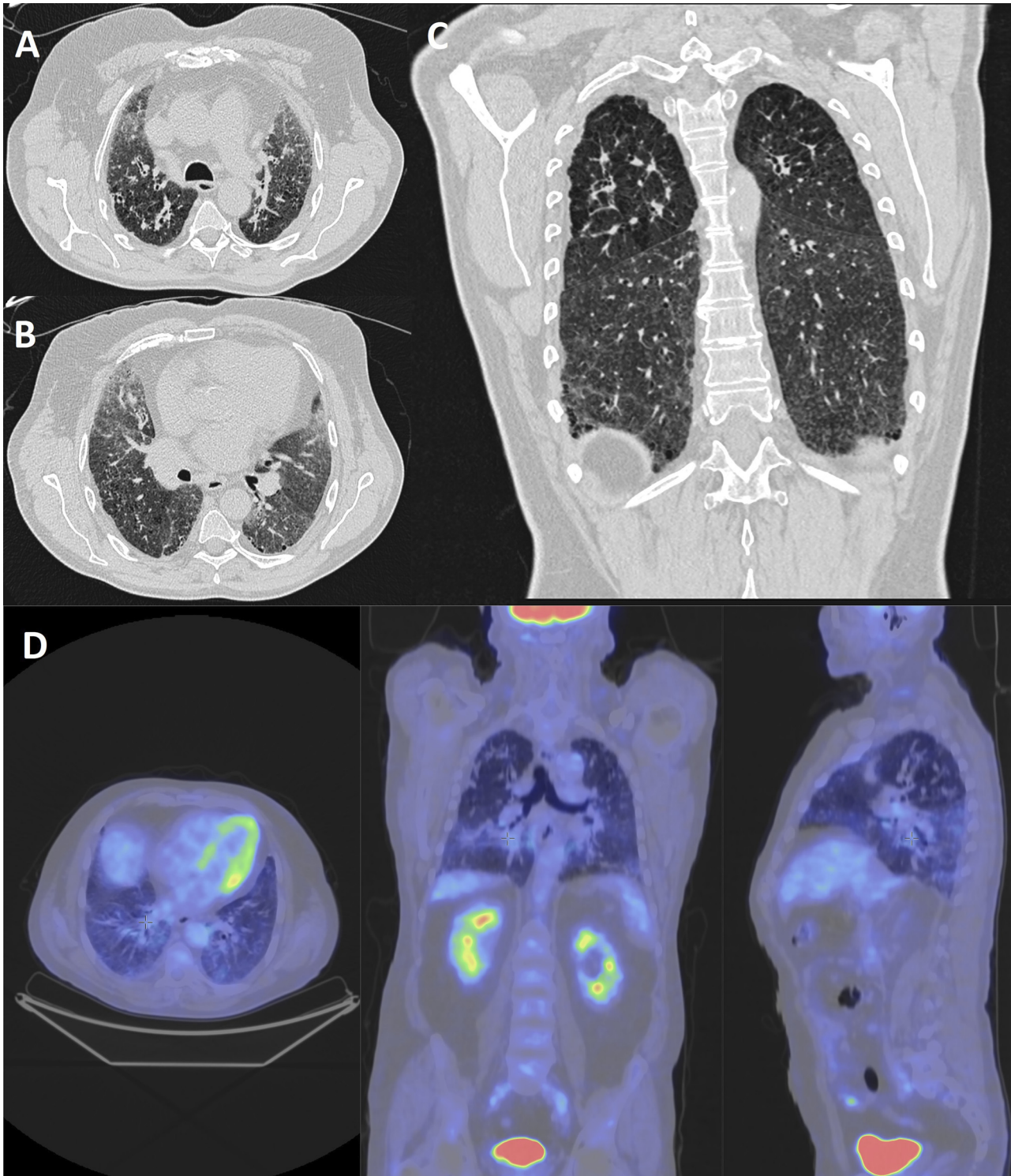


Fig. 1. Representative example of the lung alterations of a patient with IPF. Axial cranial (a) and caudal (b) level, and coronal (c) HRCT images of a 61 year-old patient with IPF. UIP-pattern of fibrosis characterized by honeycombing cysts and reticular septal thickening with subpleural and basal dominance. Fluorodeoxyglucose avidity is apparent on PET (d). The lung parenchymal honeycombing identified on the HRCTs is associated with increased ^{18}F -FDG uptake

can be associated with areas of architectural distortion [13]. Due to these increased linear densities, some degree of architectural distortion may lead to one or two airways being held open, giving rise to traction bronchiectasis. The

presence or absence of traction bronchiectasis is very important. On its own it does not mean definite UIP. These are the dilated airways being held open, an important marker of fibrosis. In an axial plane, a round area of

Table 2. HRCT criteria for UIP [4]

UIP pattern	Probable UIP pattern	Indeterminate for UIP pattern	Alternative Diagnosis
<ul style="list-style-type: none"> -Subpleural, basal predominance; distribution is often heterogeneous -Reticular abnormality -Honeycombing with or without peripheral traction bronchiectasis or bronchiolectasis -Absence of features listed as <u>inconsistent with UIP pattern (see third column)</u> 	<ul style="list-style-type: none"> -Subpleural, basal predominance; distribution is often heterogeneous -Reticular pattern with peripheral traction bronchiectasis or bronchiolectasis -May have mild ground-glass opacity (GGO) 	<ul style="list-style-type: none"> -Subpleural and basal predominance -Subtle reticulation; may have mild GGO or distortion (“early UIP pattern”) -CT features and/or distribution of lung fibrosis that do not suggest any specific etiology (“truly indeterminate for UIP”) 	<p>Findings suggestive of another diagnosis, including:</p> <p style="text-align: center;"><u>CT features</u></p> <ul style="list-style-type: none"> -Cysts -Marked mosaic attenuation -Predominant GGO -Profuse micronodules -Centrilobular nodules -Nodules -Consolidation <p style="text-align: center;"><u>Predominant distribution:</u></p> <ul style="list-style-type: none"> -Peribronchovascular -Perilymphatic -Upper or mid-lung <p style="text-align: center;"><u>Other:</u></p> <ul style="list-style-type: none"> -Pleural plaques (consider asbestosis) -Dilated esophagus (consider CTD) -Distal clavicular erosions (consider RA) -Extensive lymph node enlargement (consider other etiologies) -Pleural effusions, pleural thickening (consider CTD/drugs)

Abbreviations: CT = computed tomography; CTD = connective tissue disease; GGO = ground-glass opacities; RA = rheumatoid arthritis; UIP = usual interstitial pneumonia.



Table 3. Histopathological criteria for UIP pattern [4]

UIP pattern	Probable UIP pattern	Intermediate for UIP pattern	Alternative Diagnosis
<ul style="list-style-type: none"> -Dense fibrosis with architectural distortion (i.e., destructive scarring and/or honeycombing) -Predominant subpleural and/or paraseptal distribution of fibrosis -Patchy involvement of lung parenchyma by fibrosis -Fibroblast foci - Absence of features to suggest an alternate diagnosis 	<ul style="list-style-type: none"> -Some histologic features from column 1 are present but to an extent that precludes a definite diagnosis of UIP/IPF And - Absence of features to suggest an alternative diagnosis <p style="text-align: center;">Or</p> <ul style="list-style-type: none"> - Honeycombing only 	<ul style="list-style-type: none"> -Fibrosis with or without architectural distortion, with features favoring either a pattern other than UIP or features favoring UIP secondary to another cause -Some histologic features from column 1, but with other features suggesting an alternative diagnosis 	<ul style="list-style-type: none"> -Features of other histologic patterns of IIPs (e.g., absence of fibroblast foci or loose fibrosis) in all biopsies -Histologic findings indicative of other diseases (e.g., hypersensitivity pneumonitis, Langerhans cell histiocytosis, sarcoidosis, LAM)

Abbreviations: IIP = idiopathic interstitial pneumonia; IPF = idiopathic pulmonary fibrosis; LAM = lymphangioleiomyomatosis; UIP = usual interstitial pneumonia.

lucency may be seen instead, with the airway marked by an adjacent vessel. Although it is a good marker of underlying pulmonary fibrosis, it is seen in other diseases as well, such as non-specific interstitial pneumonia (NSIP) [14]. In a study conducted by Walsh et al. on 162 patients with histologic diagnosis of UIP or NSIP, the severity of traction bronchiectasis on HRCT was correlated to higher fibroblastic foci profusion in UIP patients, but not in NSIP patients. These key findings of UIP pattern with fibroblastic foci predict physiologic decline and mortality. Since traction bronchiectasis is an independent surrogate marker for fibroblastic foci profusion seen histologically, it can thus predict disease prognosis [15].

Honeycombing, another important diagnostic criterion, is characterized by various cystic airspaces encompassed by thick fibrous walls, representing destroyed and fibrotic lung tissue [13]. In a coronal image, it is classical to see a basal predominance, with a subpleural and peripheral distribution, often being symmetrical. Hexagonal, isolated or clustered subpleural cysts can be seen in a single axial cut, possibly causing some architectural distortion. The cysts resemble a honeycomb, which are found to measure from 2 mm to 2 cm in diameter. The shape, distribution and location are critical in identifying honeycombing. A single or two cyst layers are sufficient to diagnose the subpleural cystic disease.

The hallmark for assessing and monitoring restrictive lung diseases is the pulmonary function test (PFT) parameter TLC. However, FVC has been commonly used as an indicator of disease severity. Most studies only use spirometric measurements and do not include body-plethysmography. Hasti et al. conducted a study with 273 IPF patients correlating CT-evaluated lung volumes and PFT parameters. Lung height, aortosternal distance, and oblique fissure retraction distance, were three reproducible automated CT surrogate measurements used to calculate the lung volume parameters on a held full inspiration. The lung volume, and the height of lung measured by HRCT were significantly related to PFT-derived parameters independent from fibrosis and emphysema. A strong inverse correlation was seen between CT-derived lung height and FVC. This is because IPF patients tend to have fibrosis of the lower lungs, resulting in a cranial displacement of the diaphragm and therefore a lung height reduction [16].

Quantitative computed tomography

HRCT is an essential tool in defining an *in vivo* perspective of pattern, extent and distribution of lung parenchyma abnormalities. Quantitative CT has the ability to illustrate features that may not be visually recognized. Specific pattern characteristics of abnormality labeled by trained IPF experts are extracted and incorporated into an automated textural analysis. This in turn creates a machine-learning algorithm which is designed to predict specific CT patterns [17]. Due to confounding intra- and inter-observer

variability, the quantification of HRCT with a computer-aided quantitative scoring, may aid in a more reproducible assessment of parenchymal lung abnormalities [18]. Quantitative CT pattern recognition software has the power to decrease, but not eliminate, the inter-observer discrepancies when diagnosing [19, 20]. They incorporate different domains of the disease, which have been demonstrated to be reproducible. The finer composite measurements try to increase the accuracy and sensitivity of disease prognosis and severity stratification in patients with IPF [18]. By increasing the precision of quantification of the disease, it has the potential to further refine patients who should be included in specific treatment trials [17]. With composite measures, IPF severity and progression could be more accurately assessed.

There are different types of quantitative CT analyses used, namely the density histogram analysis, the density mask analysis, texture classification analysis and mean CT value of the whole lungs. The texture classification analysis method has evidence showing it as the most reliable and useful in managing IPF patients.

In the 1980's the first computer-based CT image analysis algorithm was developed to analyze the mean CT value of whole lungs in interstitial lung disease [21]. Best et al., in a study of 167 IPF patients, used density histograms to calculate CT values of the mean whole lungs, the skewness (asymmetry), and kurtosis (peakedness). These histogram-based measurements, when compared to physiological measures such as FVC, were shown to have a moderate link in describing the progression and severity of the disease [17, 22]. Greater extents of fibrosis were associated with lower TLC, skewness and kurtosis values [22].

For example, the serial assessment of HRCT quantification is able to quantify subtle changes in fibrotic intensity, which may not be visible otherwise to the human eye. Based on unique HRCT texture patterns for honeycombing, GGO, and reticular fibrosis with architectural distortion, a computer-aided system is used to quantify IPF fibrotic changes. Reticular fibrosis and total fibrosis were shown to be predictive of survival [19].

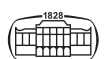
Multidetector CT (MDCT) is another alternative to assessing the progression of the disease *in vivo* with the ability to identify features that may not be visually recognizable. Colombi et al. found a novel density histogram analysis method, which uses percentiles to identify disease progression. The study concluded that the 40th percentile density histogram might reflect changes in the overall extent of lung abnormalities, while the 80th percentile may illustrate changes in reticular opacities. Both of these values correlate with pulmonary function test and radiologists visual scores [23].

Density mask technique, initially developed to quantify emphysema in patients with COPD, is a method that uses two thresholds [24]. Its objective is to assess the severity and progression of patients with IPF using quantitative-CT measurements and lung physiology. The attenuation (in Hounsfield unit (HU)) of IPF lungs strongly correlates with FVC in determining severity and progression. Ohkubo et al. by using a volumetric analysis density mask technique

quantified fibrotic changes in interstitial pneumonia based on levels of attenuation. A normal attenuated lung was defined as the area between -950 and -701 HU, correlating with FVC. Regions of higher attenuation (>-701 HU) were seen as areas of ground-glass attenuation and consolidation, and lower attenuation (<-950 HU) as areas of emphysema. Since the lung attenuation strongly correlated with FVC, it is an important finding for those patients who may not be able to perform a PFT and can instead rely on CT analysis to determine the severity [25].

As previously mentioned, FVC and DL_{co} are strong indicators to interpret the extent of the disease. Unfortunately, severe IPF patients may not be able to perform a PFT. In addition, these PFT findings can also be confounded in patients with coexisting emphysema. In fact, emphysema is present in approximately one-third of IPF patients [26]. In a study performed by Gibson et al. on patients suffering from ILD, it was found that patients exhibiting typical UIP pattern on HRCT were commonly seen as COPD/emphysema patients [27]. Nakagawa et al. was able to develop a density mask technique that extracted honeycombing areas on CT images based on both low attenuation areas and areas of low attenuation surrounded by thick walls. This technique was successfully able to differentiate IPF with emphysema, which has low attenuation surrounded by thin walls. This gives importance to the clinical usefulness of being able to quantify honeycombing areas. The percent honeycombing (HA) was an independent predictor of mortality, with patients showing $HA \geq 4.8\%$ having lower survival rates. The honeycombing areas were also associated with decreased FVC, composite physiologic index (CPI) and fibrotic areas identified with visual score by radiologists. They show consistency with visual assessment and provide clear cut-off points [26].

Quantitative computer-derived (CAD) CT measurements study lung parenchyma features that have no visual correlations. A CAD based on CT-generated volumetric data was initially developed to detect interstitial lung diseases. Zavaletta further continued to develop this method by integrating texture matching techniques to differentiate lung regions into 5 classes: normal, ground-glass, reticular, honeycombing, and emphysema [28]. Similar textural analysis methods have been developed since then, which have also shown some clinical usefulness in assessment. Park et al. found that assessing disease severity in UIP and NSIP patients was possible with an automated volumetric quantification of HRCT patterns in normal, GGO and honeycombing lung regions [29]. The Computer-Aided Lung Informatics for Pathology Evaluation and Rating (CALIPER) method, an automated volumetric tool used to quantify and analyze lung parenchyma abnormality features on HRCT, is based on Zavaletta's method and is widely used today. Moldonado et al. illustrated with CALIPER quantification that changes in reticular opacity and honeycombing correlated with physiologic parameters, which in turn are predictive with IPF patient's survival [19]. By using CALIPER software, CT measures of baseline disease severity, specifically vessel-related structures (VRSs), were shown to



predict patient's survival and FVC decline. It also proved to identify those patients who would benefit most by reaching antifibrotic trial endpoint, reducing the drug trial population by 25% [30]. Jacob et al. found that the CALIPER texture classification system was superior to CT visual scoring by radiologists in correlating pulmonary function and prognosis [31].

Salisbury et al. also characterized interstitial findings on HRCT in IPF patients using alternative textural analysis software, adaptive multiple features method (AMFM). It was seen that the fibrosis extent in AMFM, measured with ground-glass reticular scoring, was related independently to the risk of disease progression and mortality [32]. Another method based on texture classification is called the Gaussian Histogram Normalized Correlation (GHNC) system. This system compares the CT attenuation values and local histograms by dividing the lungs into 5 categories: normal, GGO, consolidation, emphysema, and fibrosis patterns. It was found to be useful in the evaluation of efficacy of patients undergoing pirfenidone treatment [33].

Christe et al. assessed the performance of the sequential INTACT CAD system using automatic classifications of HRCT images. This was achieved sequentially by segmenting the anatomical structures of the lungs, identifying and characterizing the types of pathological lung tissues, which resulted in a recommended diagnosis. The pathological lung tissues are characterized into reticulation, honeycombing, GGO, consolidation, micronodules, and normal lungs. It was found that the INTACT system had similar accuracy to a human reader in classifying IPF. These methods can be of essential use clinically, especially for those patients who may not be able to undergo SLB due to associated risks [34].

Texture-based features used by quantitative analysis, contain granular spatial information, which provide a reproducible characterization method of lung texture, contributors of different textures, and its patterns of distribution. Kim et al. demonstrated the extent of the disease in a study of 57 IPF patients with quantified lung fibrosis scores, representing reticular fibrosis with architectural distortion on CTs. At month 6, it correlated to a predicted FVC decline at month 18. CT quantification measures of lung density (kurtosis) were shown to predict mortality, but not functional changes [35].

Lastly, lung compliance can be useful in early imaging for patients with pulmonary fibrosis. Lung compliance is the quantification of lung motion when breathing. Areas of decreased lung compliance can be seen when comparing CT images during inspiration and expiration. A decline in basilar lung compliance was seen after 6 months and a decline in apical lung compliance was seen between 6 and 12 month imaging [36].

These all illustrate the significant importance quantitative lung fibrosis assessments can have in determining the severity and progression of the disease in IPF patients. Although in a clinical practice this method is useful, reproducible and less time-consuming, it remains unclear

how the methods employed achieve the specific CT index used for the texture classification algorithms.

Ultrasound

HRCT as noted, is the main standard diagnostic feature of IPF. However, it must be highlighted that during imaging, a patient is exposed to radiation [37]. Lung ultrasound (LUS) is a noninvasive method that is sensitive in detecting changes in the subpleural space. This is portrayed as a thick, irregular fragmented pleura line when a fibrotic scar is present. Moreover, it can also differentiate upper and basal predominance of fibrosis [38]. Higher frequency probes of 8–11 MHz are able to characterize the pleural line thickness [39, 40].

In interstitial lung diseases, diffuse, multiple B-lines described as vertical hyperechoic artifacts can be seen. The number of B-lines is correlated to the severity and extent of fibrosis seen on HRCT. Since LUS is a repeatable and noninvasive procedure, it can be a useful imaging method to monitor the progression of IPF disease [38].

Parenchymal alterations can be seen because of alveolar air loss and the presence or absence of interstitial fluids [41]. Due to an unaltered alveolar space with thin interlobular septa, an acoustic barrier is created by air, resulting in an interface between the pleura and the chest wall's soft tissue. This in turn is portrayed as a difference in acoustic impedance [42]. A-lines, also called the "mirror effect," are the chest wall's reflections below the pleural line [43], characterized by horizontal lines seen at constant intervals in areas of artifacts, such as increased subpleural air seen in emphysema or honeycombing. These in turn can be prognostic features in assessing the severity of IPF [39]. Multiple A lines and a blurred pleura line were used to describe severe forms of pulmonary fibrosis. Multiple A lines have been introduced to describe parallel artifacts arising from the pleural line, seen subpleurally running to the edge of the screen, with a wide base and a narrow top. They were shown to be located in the same areas HRCT portrayed honeycombing and subpleural cysts. The blurred pleural line indicated a positive correlation with honeycombing in HRCT [39].

B-lines, on the other hand, are long and well-defined hyperechoic artifacts, arising from the pleural line. They are due to thickened subpleural interlobular septa seen in between lung intercostal spaces (LIS). Sperandoe et al. noted a greater amount of B-lines in moderate or severe forms of IPF, along with a thickened irregular >3 mm pleural line [44]. In an extended study, it was concluded that a pleural line ≥ 5 mm was seen in severe IPF [40]. If there are >10 B-lines per LIS, extravascular water in the alveolar compartments is suspected [45]. A "white lung" occurs when multiple B-lines merge together generating one vertical artifact, modeled in HRCT as GGO, and corresponding with inconsistent UIP pattern [46]. Normally, the pleural line is seen as a horizontal hyperechoic line half a centimeter below



the rib line. Patients with fibrotic lungs have a thickened irregular line, >3 mm thick, due to subpleural abnormalities. If three B line artifacts arise from the pleural line with <7 mm between two lines, interstitial syndrome such as reticulation and honeycombing can be described. This appears as a “long rocket” [47]. By simply measuring the distance between two B-lines, alveolar and interstitial syndromes can be differentiated. Based on the thickness of the pleural line, LUS can differentiate cardiogenic and fibrotic interstitial syndromes [48].

With the use of LUS, the number of B-lines and the distance between them can distinguish alveolar syndrome and interstitial syndrome, while the thickness of the pleural line can assess the severity of IPF. Both of them correlate to the extension of fibrosis seen in HRCT. Certainly, the fibrotic pattern can only be clarified by HRCT.

Magnetic resonance imaging

The role of magnetic resonance imaging (MRI) in the diagnosis and management of IPF is still under investigation. In MRI, subpleural and paraseptal fibrosis can be seen along with honeycombing next to unaffected lung parenchyma. Late-enhanced MRI shows significant contrast enhancement in fibrotic lung tissue. Mirsadraee et al. performed a study with 10 IPF and 10 control patients, examining T1 mapping (relaxation phenomena) at 3T MRI. On a single pre-selected HRCT slice, MRI modified look-locker inversion recovery (MOLLI) sequence was performed during a 15–20 s breath hold. The observers were able to visualize a higher T1 pre-contrast in fibrotic lungs. Moreover, a delayed uptake of contrast agent was detected in fibrotic lungs. Although the study population was small, MRI proved to be a great tool in differentiating between normal and fibrotic lungs, as well as detecting early fibrosis and assessing its activity that may not be visible on CT [49]. However, although MRI is a radiation free technique, it also comes with some disadvantages. MRI is a less sensitive method, with thick collimation (8 mm compared to 1–1.25 mm in HRCT), which does not allow precise anatomical evaluation of interstitial changes. It is often very difficult for IPF patients to perform long breath holds and remain still, limiting MRI usage in a clinical setting as well [50].

Positron emission tomography

Identification of early IPF may be possible with the use of positron emission tomography (PET) scan. Groves et al. illustrated the relationship between mean maximal standard uptake value (SUV_{max}) and lung functional parameters (FVC and DL_{CO}). In a study of 36 patients, of which 18 were IPF patients, areas with higher reticulation and honeycombing (SUV_{max} 3.0 ± 1.0) in HRCT had increased metabolism of ^{18}F -fluorodeoxyglucose (^{18}F -FDG) than regions of higher ground-glass opacification (SUV_{max}). This can be

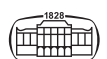
seen in Fig. 1. The metabolism was measured as a standardized uptake value (SUV_{max} 2.0 ± 0.4). Based on the uptake of ^{18}F -FDG, it is possible to predict measurements of lung physiology in these patients to discriminate different degrees of disease severity [51].

Umeda et al. studied dual-time point ^{18}F -FDG PET imaging in 50 IPF patients. The time points were at 60 and 180 min from the time of ^{18}F -FDG injection. Two weeks prior to the dual-time point ^{18}F -FDG PET, patients underwent a HRCT. From the region-of-interest on the HRCT, the SUV was measured after the ^{18}F -FDG injection, and the retention index value (RI-SUV) was calculated between the early and delayed imaging. These values were further compared to pulmonary function tests in every patient after a 6-month follow-up time. Higher RI-SUV values and a higher extent of fibrosis were proven to be independent predictors of short progression-free survival. A RI-SUV cut off value of 1.5 or greater, with a sensitivity, specificity and accuracy of 90.3, 94.3, and 93.5% respectively, was established to be able to predict long-term prognosis. Higher RI-SUV values and lower FVC values were shown to be independent predictors of overall survival rate and mortality. Based on these results, ^{18}F -FDG PET imaging could serve as a valuable tool in assessing the risk of mortality, prioritizing patients waiting for lung transplantation [52].

Recent evidences have shown that macrophages and monocytes play a role in the progression of IPF. Withana et al. developed a bimodal optical/PET activity-based probe (ABP) to monitor the pathophysiology of IPF. The optical analysis allows for *in vivo* and *in vitro* monitoring. Cysteine cathepsin-targeted imaging probes were used to specifically monitor the activated pools of immune cells, suggesting that clinical PET imaging has potential to generate molecular information responsible for influencing the severity and progression of IPF. Gallium-68 (^{68}Ga) was used as the radionuclide in the first human trials. This finding is important as it might allow for an earlier diagnosis of IPF with increased sensitivity when compared to HRCT. Its non-invasive imaging also shows an increased uptake of cysteine cathepsin activity in fibrotic lesions, suggesting the role of activated macrophages [53].

Conclusion

The rising incidence and prevalence of IPF, in association with its poor prognosis, has drawn attention to the importance of its early recognition and diagnosis using imaging modalities. HRCT has become the gold standard imaging modality for diagnosing IPF. To improve the recognition of the disease, collaborative guidelines by ATS, ERS, JPS, and ALAT have delineated histopathological and HRCT criteria in diagnosing UIP. HRCT quantitative lung fibrosis assessments can have substantial importance in determining the severity and progression of IPF. Other imaging techniques, which do not show an equivalent diagnostic potential as HRCT and are not as commonly used in practice, include



LUS, MRI and PET-CT. An integrated MDD approach in the diagnosis of IPF, could lead to an earlier detection of the disease, allowing a decline of its progression.

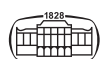
Funding sources: Thematic Excellence Programme (2020-4.1.1.-TKP2020) of the Ministry for Innovation and Technology in Hungary, within the framework of the Therapeutic Development and Bioimaging thematic programmes of the Semmelweis University.

REFERENCES

- [1] Raghu G, Collard HR, Egan JJ, Martinez FJ, Behr J, Brown KK, et al.: An Official ATS/ERS/JRS/ALAT Statement: idiopathic pulmonary fibrosis: evidence-based guidelines for diagnosis and management. *Am J Respir Crit Care Med* 2011; 183(6): 788–824. <https://doi.org/10.1164/rccm.2009-040GL>.
- [2] Provencher D, Jauregui A: Recommendations for evaluating and managing idiopathic pulmonary fibrosis. *J Am Acad Phys. Assist* 2018; 31(9): 21–6. <https://doi.org/10.1097/01.JAA.0000544299.00459.a4>.
- [3] Raghu N, Anstrom K, King T, Lasky J, Martinez F, Idiopathic Pulmonary Fibrosis Clinical Research: Prednisone, azathioprine, and N-acetylcysteine for pulmonary fibrosis. *N Engl J Med* 2012; 366(21): 1968–77. <https://doi.org/10.1056/NEJMoa1113354>.
- [4] Raghu G, Remy-Jardin M, Myers JL, Richeldi L, Ryerson CJ, Lederer DJ, et al.: Diagnosis of idiopathic pulmonary fibrosis an Official ATS/ERS/JRS/ALAT Clinical practice guideline. *Am J Respir Crit Care Med* 2018; 198(5): e44–68. <https://doi.org/10.1164/rccm.201807-1255ST>.
- [5] Martinez F, Collard H, Pardo A, Raghu G, Richeldi L, Selman M, et al.: Idiopathic pulmonary fibrosis. *Nat Rev Dis Primers* 2017. <https://doi.org/10.1038/nrdp.2017.74>.
- [6] Hutchinson J, Fogarty A, Hubbard R, McKeever T: Global incidence and mortality of idiopathic pulmonary fibrosis: a systematic review. *Eur Respir J* 2015; 46(3): 795–806. <https://doi.org/10.1183/09031936.00185114>.
- [7] King T, Albera JC, Bradford WZ, Costabel U, du Bois RM, Leff JA, et al.: All-cause mortality rate in patients with idiopathic pulmonary fibrosis: implications for the design and execution of clinical trials. *Am J Respir Crit Care Med* 2014; 189(7): 825–31. <https://doi.org/10.1164/rccm.201311-1951OC>.
- [8] Kreuter M, Ehlers-Tenenbaum S, Palmowski K, Bruhwylter J, Oltmanns U, Muley T, et al.: Impact of comorbidities on mortality in patients with idiopathic pulmonary fibrosis. *PLoS One* 2016; 11(3): e0151425. <https://doi.org/10.1371/journal.pone.0151425>.
- [9] Tran T, Sterclova M, Mogulkoc N, Lewandowska K, Muller V, Hajkova M, et al.: The European MultiPartner IPF registry (EMPIRE): validating long-term prognostic factors in idiopathic pulmonary fibrosis. *Respir Res* 2020; 21(1): 11. <https://doi.org/10.1186/s12931-019-1271-z>.
- [10] King TE, Pardo A, Selman M: Idiopathic pulmonary fibrosis. 2011. [https://doi.org/10.1016/S0140-6736\(11\)60052-4](https://doi.org/10.1016/S0140-6736(11)60052-4).
- [11] Jo H, Glaspole I, Grainge C, Goh N, Hopkins P, Moodley Y, et al.: Baseline characteristics of idiopathic pulmonary fibrosis: analysis from the Australian idiopathic pulmonary fibrosis registry. *Eur Respir J* 2017; 49(2). <https://doi.org/10.1183/13993003.01592-2016>.
- [12] Raghu G, Remy-Jardin M, Myers J, Richeldi L, Wilson K: The 2018 diagnosis of idiopathic pulmonary fibrosis guidelines: surgical lung biopsy for radiological pattern of probable usual interstitial pneumonia is not mandatory. *Am J Respir Crit Care Med* 2019. <https://doi.org/10.1164/rccm.201907-1324ED>.
- [13] Hansell DM, Bankier AA, MacMahon H, McLoud TC, Müller NL, Remy J: Fleischner Society: glossary of terms for thoracic imaging. *Radiology* 2008. <https://doi.org/10.1148/radiol.2462070712>.
- [14] Lynch D, Sverzellati N, Travis W, Brown K, Colby T, Galvin J, et al.: Diagnostic criteria for idiopathic pulmonary fibrosis: a Fleischner society white paper. *The Lancet Respir Med* 2018. [https://doi.org/10.1016/S2213-2600\(17\)30433-2](https://doi.org/10.1016/S2213-2600(17)30433-2).
- [15] Walsh S, Wells A, Sverzellati N, Devaraj A, von der Thusen J, Yousem S, et al.: Relationship between fibroblastic foci profusion and high resolution CT morphology in fibrotic lung disease. *BMC Med* 2015; 13: 241. <https://doi.org/10.1186/s12916-015-0479-0>.
- [16] Robbie H, Wells A, Jacob J, Walsh S, Nair A, Srikanthan A, et al.: Visual and automated CT measurements of lung volume loss in idiopathic pulmonary fibrosis. *Am J Roentgenol* 2019; 213(2): 318–24. <https://doi.org/10.2214/AJR.18.20884>.
- [17] Hansell DM, Goldin JG, King TE, Lynch DA, Richeldi L, Wells AU: CT staging and monitoring of fibrotic interstitial lung diseases in clinical practice and treatment trials: a Position Paper from the Fleischner society. *The Lancet Respir Med* 2015. [https://doi.org/10.1016/S2213-2600\(15\)00096-X](https://doi.org/10.1016/S2213-2600(15)00096-X).
- [18] Lammi M, Baughman R, Biring S, Russell A, Ryu J, Scholand M, et al.: Outcome measures for clinical trials in interstitial lung diseases. *Curr Respir Med Rev* 2015; 11(2): 163–74. <https://doi.org/10.2174/1573398x11666150619183527>.
- [19] Maldonado F, Moua T, Rajagopalan S, Karwoski R, Raghunath S, Decker P, et al.: (2014). Automated quantification of radiological patterns predicts survival in idiopathic pulmonary fibrosis. *Eur Respir J*. <https://doi.org/https://doi.org/10.1183/09031936.00071812>.
- [20] Jacob J, Bartholmai B, Rajagopalan S, Kokosi M, Nair A, Karwoski R, et al.: Automated quantitative computed tomography versus visual computed tomography scoring in idiopathic pulmonary fibrosis validation against pulmonary function. *J Thorac Imaging* 2016; 31(5): 304–11. <https://doi.org/10.1097/RTI.0000000000000220>.
- [21] Gilman M, Laurens R, Somogyi J, Honig E: CT attenuation values of lung density in sarcoidosis. *J Comput Assist Tomogr* 1983; 7(3): 407–10. <https://doi.org/10.1097/00004728-198306000-00003>.
- [22] Best A, Meng J, Lynch A, Bozic C, Miller D, Grunwald G, et al.: Idiopathic pulmonary fibrosis: physiologic tests, quantitative CT indexes, and CT visual scores as predictors of mortality. *Radiology* 2008; 246(3): 935–40. <https://doi.org/10.1148/radiol.2463062200>.
- [23] Colombi D, Dinkel J, Weinheimer O, Obermayer B, Buzan T, Nabers D, et al.: Research Article: Visual vs fully automatic histogram-based assessment of idiopathic pulmonary fibrosis (IPF) progression using sequential multidetector computed



- tomography (MDCT). *PLoS One* 2015; 10(6): e0130653. <https://doi.org/10.1371/journal.pone.0130653>.
- [24] Wang Z, Gu S, Leader J, Kundu S, Tedrow J, Sciruba F, et al.: Optimal threshold in CT quantification of emphysema. *Eur Radiol* 2013; 23(4): 975–84. <https://doi.org/10.1007/s00330-012-2683-z>.
- [25] Ohkubo H, Kanemitsu Y, Uemura T, Takakuwa O, Takemura M, Maeno K, et al.: Normal lung quantification in usual interstitial pneumonia pattern: the impact of threshold-based volumetric CT analysis for the staging of idiopathic pulmonary fibrosis. *PLoS One* 2016; 11(3): e0152505. <https://doi.org/10.1371/journal.pone.0152505>.
- [26] Nakagawa H, Ogawa E, Fukunaga K, Kinose D, Yamaguchi M, Nagao T, et al.: Quantitative CT analysis of honeycombing area predicts mortality in idiopathic pulmonary fibrosis with definite usual interstitial pneumonia pattern: a retrospective cohort study. *PLoS One* 2019; 14(3): e0214278. <https://doi.org/10.1371/journal.pone.0214278>.
- [27] Gibson C, Bhatt A, Deshwal H, Li X, Goldberg J, Ko J, et al.: Comparison of clinical measures among interstitial lung disease (ILD) patients with usual interstitial pneumonia (UIP) patterns on high-resolution computed tomography. *Lung* 2020; 198(5): 811–9. <https://doi.org/10.1007/s00408-020-00387-6>.
- [28] Zavaletta V, Bartholmai B, Robb R: High resolution multidetector CT-aided tissue analysis and quantification of lung fibrosis. *Acad Radiol* 2007; 14(7): 772–87. <https://doi.org/10.1016/j.acra.2007.03.009>.
- [29] Park S, Seo J, Kim N, Lee Y, Lee J, Kim D: Comparison of usual interstitial pneumonia and nonspecific interstitial pneumonia: quantification of disease severity and discrimination between two diseases on HRCT using a texture-based automated system. *Korean J Radiol* 2011; 12(3): 297–307. <https://doi.org/10.3348/kjr.2011.12.3.297>.
- [30] Jacob J, Bartholmai B, Rajagopalan S, van Moorsel C, van Es H, van Beek F, et al.: Predicting outcomes in idiopathic pulmonary fibrosis using automated computed tomographic analysis. *Am J Respir Crit Care Med* 2018; 198(6): 767–76. <https://doi.org/10.1164/rccm.201711-2174OC>.
- [31] Jacob J, Bartholmai B, Rajagopalan S, Kokosi M, Nair A, Karwoski R, et al.: Mortality prediction in idiopathic pulmonary fibrosis: evaluation of computer-based CT analysis with conventional severity measures. *Eur Respir J* 2017; 49(1). <https://doi.org/10.1183/13993003.01011-2016>.
- [32] Salisbury M, Lynch D, van Beek E, Kazerooni E, Guo J, Xia M, et al.: Idiopathic pulmonary fibrosis: the association between the adaptive multiple features method and fibrosis outcomes. *Am J Respir Crit Care Med* 2017; 195(7): 921–9. <https://doi.org/10.1164/rccm.201607-1385OC>.
- [33] Iwasawa T, Ogura T, Sakai F, Kanauchi T, Komagata T, Baba T, et al.: CT analysis of the effect of pirfenidone in patients with idiopathic pulmonary fibrosis. *Eur J Radiol* 2014; 83(1): 32–8. <https://doi.org/10.1016/j.ejrad.2012.02.014>.
- [34] Christe A, Peters A, Drakopoulos D, Heverhagen J, Geiser T, Stathopoulou T, et al.: Computer-aided diagnosis of pulmonary fibrosis using deep learning and CT images. *Invest Radiol* 2019; 54(10): 627–32. <https://doi.org/10.1097/RLI.0000000000000574>.
- [35] Kim H, Brown M, Chong D, Gjertson D, Lu P, Kim H, et al.: Comparison of the quantitative CT imaging biomarkers of idiopathic pulmonary fibrosis at baseline and early change with an interval of 7 Months. *Acad Radiol* 2015; 22(1): 70–80. <https://doi.org/10.1016/j.acra.2014.08.004>.
- [36] Nair G, Castillo E: Longitudinal lung compliance imaging in idiopathic pulmonary fibrosis. *Radiology* 2019. <https://doi.org/10.1148/radiol.2019191115>.
- [37] European Commission: Radiation protection 118 Referral guidelines for imaging; 2000.
- [38] Walsh S, Calandriello L, Sverzellati N, Wells A, Hansell D, U.I.P.O. Consort: Interobserver agreement for the ATS/ERS/JRS/ALAT criteria for a UIP pattern on CT. *Thorax* 2016; 71(1): 45–51. <https://doi.org/10.1136/thoraxjnl-2015-207252>.
- [39] Buda N, Piskunowicz M, Porzezińska M, Kosiak W, Zdrojewski Z: Lung ultrasonography in the evaluation of interstitial lung disease in systemic connective tissue diseases: criteria and severity of pulmonary fibrosis – analysis of 52 patients. *Ultraschall der Medizin* 2016; 37(4): 379–85. <https://doi.org/10.1055/s-0041-110590>.
- [40] Sperandeo M, De Cata A, Molinaro F, Trovato F, Catalano D, Simeone A, et al.: Ultrasound signs of pulmonary fibrosis in systemic sclerosis as timely indicators for chest computed tomography. *Scand J Rheumatol* 2015; 44(5): 389–98. <https://doi.org/10.3109/03009742.2015.1011228>.
- [41] Volpicelli G: Lung sonography. *J Ultrasound Med* 2013. <https://doi.org/10.7863/jum.2013.32.1.165>.
- [42] Jambrik Z, Monti S, Coppola V, Agricola E, Mottola G, Miniati M, et al.: Usefulness of ultrasound lung comets as a nonradiologic sign of extravascular lung water. *Am J Cardiol* 2004; 93(10): 1265–70. <https://doi.org/10.1016/j.amjcard.2004.02.012>.
- [43] Lichtenstein DA: Lung ultrasound in the critically ill. *Ann Intensive Care* 2014. <https://doi.org/10.1186/2110-5820-4-1>.
- [44] Sperandeo M, Varriale A, Sperandeo G, Filabozzi P, Piattelli M, Carnevale V, et al.: Transthoracic ultrasound in the evaluation of pulmonary fibrosis: our experience. *Ultrasound Med Biol* 2009; 35(5): 723–9. <https://doi.org/10.1016/j.ultrasmedbio.2008.10.009>.
- [45] Picano E, Frassi F, Agricola E, Gligorova S, Gargani L, Mottola G: Ultrasound lung comets: a clinically useful sign of extravascular lung water. *J Am Soc Echocardiography* 2006. <https://doi.org/10.1016/j.echo.2005.05.019>.
- [46] Copetti R, Soldati G, Copetti P: Chest sonography: a useful tool to differentiate acute cardiogenic pulmonary edema from acute respiratory distress syndrome. *Cardiovasc Ultrasound* 2008; 6: 16. <https://doi.org/10.1186/1476-7120-6-16>.
- [47] Volpicelli G, Elbarbary M, Blaivas M, Lichtenstein D.A, Mathis G, Kirkpatrick A.W, et al.: International evidence-based recommendations for point-of-care lung ultrasound. 2012. <https://doi.org/10.1007/s00134-012-2513-4>.
- [48] Barskova T, Gargani L, Guiducci S, Randone S, Bruni C, Carnesecchi C, et al.: Lung ultrasound for the screening of interstitial lung disease in very early systemic sclerosis. *Ann Rheum Dis* 2013; 72(3): 390–5. <https://doi.org/10.1136/annrheumdis-2011-201072>.
- [49] Mirsadraee S, Tse M, Kershaw L, Semple S, Schembri N, Chin C, et al.: T1 characteristics of interstitial pulmonary fibrosis on 3T MRI: a predictor of early interstitial change? *Quant Imaging Med Surg* 2016; 6(1): 42–9. <https://doi.org/10.3978/j.issn.2223-4292.2016.02.02>.



- [50] Rea G: Magnetic resonance imaging in the evaluation of idiopathic pulmonary fibrosis: a real possibility, or an attractive challenge? Quantitative Imaging Med Surg 2016. <https://doi.org/10.21037/qims.2016.06.06>.
- [51] Groves A, Win T, Sreaton N, Berovic M, Endozo R, Booth H, et al.: Idiopathic pulmonary fibrosis and diffuse parenchymal lung disease: implications from initial experience with 18F-FDG PET/CT. J Nucl Med 2009; 50(4): 538–45. <https://doi.org/10.2967/jnumed.108.057901>.
- [52] Umeda Y, Demura Y, Morikawa M, Anzai M, Kadowaki M, Ameshima S, et al.: Prognostic value of dual-time-point 18F-FDG PET for idiopathic pulmonary fibrosis. J Nucl Med 2015; 56(12): 1869–75. <https://doi.org/10.2967/jnumed.115.163360>.
- [53] Withana N, X M, McGuire H, Verdoes M, van der Linden W, Ofori L, et al.: Non-invasive imaging of idiopathic pulmonary fibrosis using cathepsin protease probes Sci Rep 2016; 6: 19755. <https://doi.org/10.1038/srep19755>.

Open Access. This is an open-access article distributed under the terms of the Creative Commons Attribution-NonCommercial 4.0 International License (<https://creativecommons.org/licenses/by-nc/4.0/>), which permits unrestricted use, distribution, and reproduction in any medium for non-commercial purposes, provided the original author and source are credited, a link to the CC License is provided, and changes - if any - are indicated.

